# Observation of an Isothermal Transformation during Quenching and Partitioning Processing

DONG H. KIM, JOHN G. SPEER, HAN S. KIM, and BRUNO C. DE COOMAN

The kinetics of the isothermal transformation, which occurs during a single-step quenching and partitioning (Q and P) process, was analyzed by means of dilatometry. Experiments revealed that an isothermal transformation with very specific characteristics occurred during the hold at the quenching temperature below the martensite start temperature. Although evidence for isothermal martensite transformation has been reported in the past for Fe-C alloys and steel, it is the first time that it is recognized to take place during the Q and P processing of low-carbon ferrous alloys.

DOI: 10.1007/s11661-009-9891-4


## I. INTRODUCTION

HIGHER strength steels with substantial ductilities can be obtained *via* the quenching and partitioning (Q and P) processing of steel with a composition similar to that of transformation-induced plasticity steel. The Q and P process has been suggested as an alternative heat treatment to produce steels with retained austenite.[1–3] Figure 1 shows a schematic for the Q and P process. The desired martensite fraction with a balanced amount of untransformed retained austenite is obtained by quenching a fully austenitic microstructure or an intercritical austenite-ferrite phase mixture to a calculated quenching temperature ($T_Q$) between the martensite start ($M_S$) temperature and martensite finish ($M_f$) temperature. The Q and P process and the method proposed to determine $T_Q$ have been reported elsewhere.[1] After the quenching step, the partitioning process is used to stabilize the austenite at room temperature by carbon partitioning from the supersaturated martensite to the interlath austenite films. If the quenched steel is partitioned at $T_Q$, the process is referred to as a one-step Q and P process. In the two-step Q and P process, the partitioning temperature is raised after quenching to a temperature close to the $M_S$ temperature.

The original Q and P processing concept is based on two important concepts: the constrained carbon equilibrium (CCE) and the athermal martensite transformation.[1–4] During quenching to $T_Q$, the martensite transformation begins at the $M_S$ temperature and proceeds only upon continuous cooling below this temperature.[4] Once the fraction of the martensite and untransformed austenite at $T_Q$ are reached, the carbon atoms partition from the supersaturated martensite to the untransformed austenite under the CCE conditions. That is, the interstitial carbon atoms partition from the martensite to the retained austenite and there is no phase boundary motion during partitioning.

In a recent dilatometric analysis of the Q and P process,[5] it was shown that the Q and P process is more complex than originally thought. One of the main findings was that an isothermal transformation occurred at the quenching temperature. Figure 2 shows the dilatometric data of the athermal martensite transformation and the isothermal transformation observed at a temperature below the $M_S$ temperature during a one-step Q and P process. After the austenitization at 950 °C for 10 minutes, the sample was quenched at a rate of −150 °C/s to avoid pearlite or bainite transformation. The dilatometric data for the continuous cooling to room temperature is consistent with the formation of athermal martensite. When the quenching was interrupted at 356 °C, *i.e.*, when the microstructure contained approximately 25 vol pct athermal martensite and 75 vol pct untransformed austenite, a clear isothermal transformation was observed at $T_Q$.

Although the isothermal martensite transformation has been observed in the past for Fe-C alloys and steel,[6] it is the first time that it has been observed to take place in low-carbon steels during the Q and P processing. In this work, the kinetics of the isothermal transformation during the single-step Q and P processing of four low C steels were examined to clarify the nature of this isothermal transformation below the $M_S$ temperature.

## II. EXPERIMENTAL

Four steels with a low hypo-eutectoid carbon content of 0.15 mass pct were used in the present work. Table I shows the composition of the steels. The Mn content was in the range of 1.5 to 2.5 mass pct to achieve a sufficient hardenability. The two CMnSi steels were

DONG H. KIM, Graduate Student, HAN S. KIM, Research Professor, and BRUNO C. De COOMAN, Professor and Director, are with the Materials Design Laboratory, Graduate Institute of Ferrous Technology, Pohang University of Science and Technology, Pohang, South Korea 790-784. Contact e-mail: decooman@postech.ac.kr JOHN G. SPEER, Professor, is with the Advanced Steel Processing and Products Research Centre, Colorado School of Mines, Golden, CO 80401.

Manuscript submitted November 11, 2008.
Article published online July 8, 2009

designed to examine the effect of Mn and Si on the isothermal transformation. The two CMnSiAl steels were used to evaluate the effect of the substitution of Si by Al on the isothermal transformation. The experiments were carried out in a Baehr 805A/D dilatometer (Baehr-Thermoanalyse GmbH, Huellhorst, Germany). Rod-type samples 10 mm in length and 3 mm in diameter were used for the dilatometry. Before the isothermal transformation heat treatment, the sample was fully austenitized at 950 °C for 1 minute and cooled to room temperature at a rate of 5 °C/s. After this normalizing treatment, the samples were heated to 950 °C and held for 10 minutes for austenitization. The heating rate was +5 °C/s. The samples were then quenched to a temperature in the range of 550 °C to 300 °C for the isothermal transformation. The cooling rate was −150 °C/s. After the heat treatment in a dilatometer, the microstructure was examined by scanning electron microscopy, Zeiss ULTRA 55 (Carl Zeiss SMT AG, Oberkochen, Germany). The sample was etched with 2 pct nital after the mechanical grinding and polishing prior to observation in the FE-SEM.

The dilatometric data were analyzed to obtain the isothermal transformation kinetics using the Johnson–Mehl–Avrami–Kolmogorov (JMAK) equation, $f_{\alpha'} = 1 - \exp(-kt^n)$. The isothermal transformation data were then plotted as $\ln\left(\ln\left(\frac{1}{1-f_{\alpha'}}\right)\right)$, as a function of $\ln t$. In this plot, the data points were found to be aligned and the slope of the straight line least-squares fitted to the data points corresponds to the $n$ parameter. The $y$ intercept is equal to $\ln k$. The calculated $n$ and $k$ parameters in the JMAK equation were then plotted as a function of the quenching temperature.

The isothermal transformation kinetics was found to differ substantially above and below the $M_S$ temperature. The results suggest that the isothermal transformation below the $M_S$ temperature is not a pure bainite transformation.

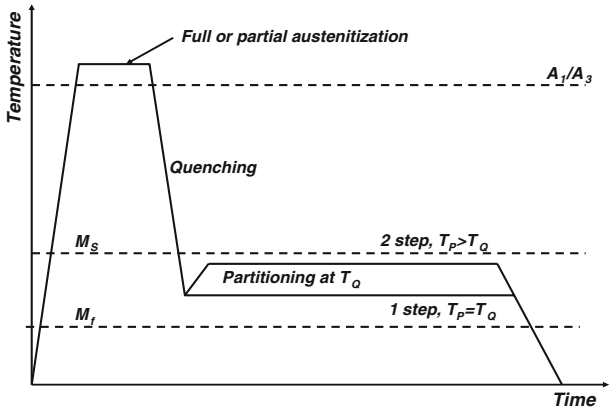


Fig. 1—Schematic of the one-step and two-step Q and P processes.

## III. RESULTS

Figure 3 shows the time-temperature-transformation (TTT) curves of the four different steels. The 0.15C1.5Mn1.4Si steel showed the fastest transformation rate in the entire temperature range. In

**Table I. Chemical Compositions of the Steels Used in the Present Work**

| Wt Pct | C | Mn | Si | Al |
|---|---|---|---|---|
| 0.15C1.5Mn1.4Si | 0.151 | 1.51 | 1.42 | 0.054 |
| 0.15C2.5Mn0.3Si | 0.152 | 2.45 | 0.30 | 0.030 |
| 0.15C2.3Mn0.5Si0.5Al | 0.153 | 2.32 | 0.55 | 0.480 |
| 0.15C2.0Mn0.3Si0.8Al | 0.149 | 2.06 | 0.32 | 0.830 |

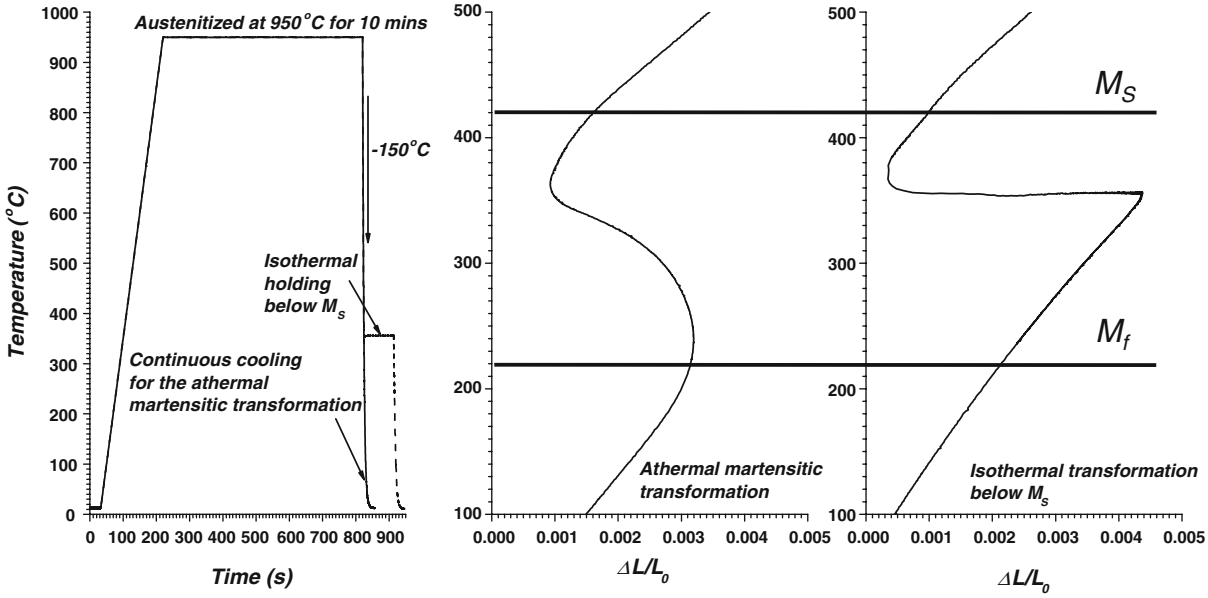


Fig. 2—Thermal cycle of continuous cooling and the corresponding dilatometry data of the athermal martensite and isothermal transformation below $M_S$ temperature.

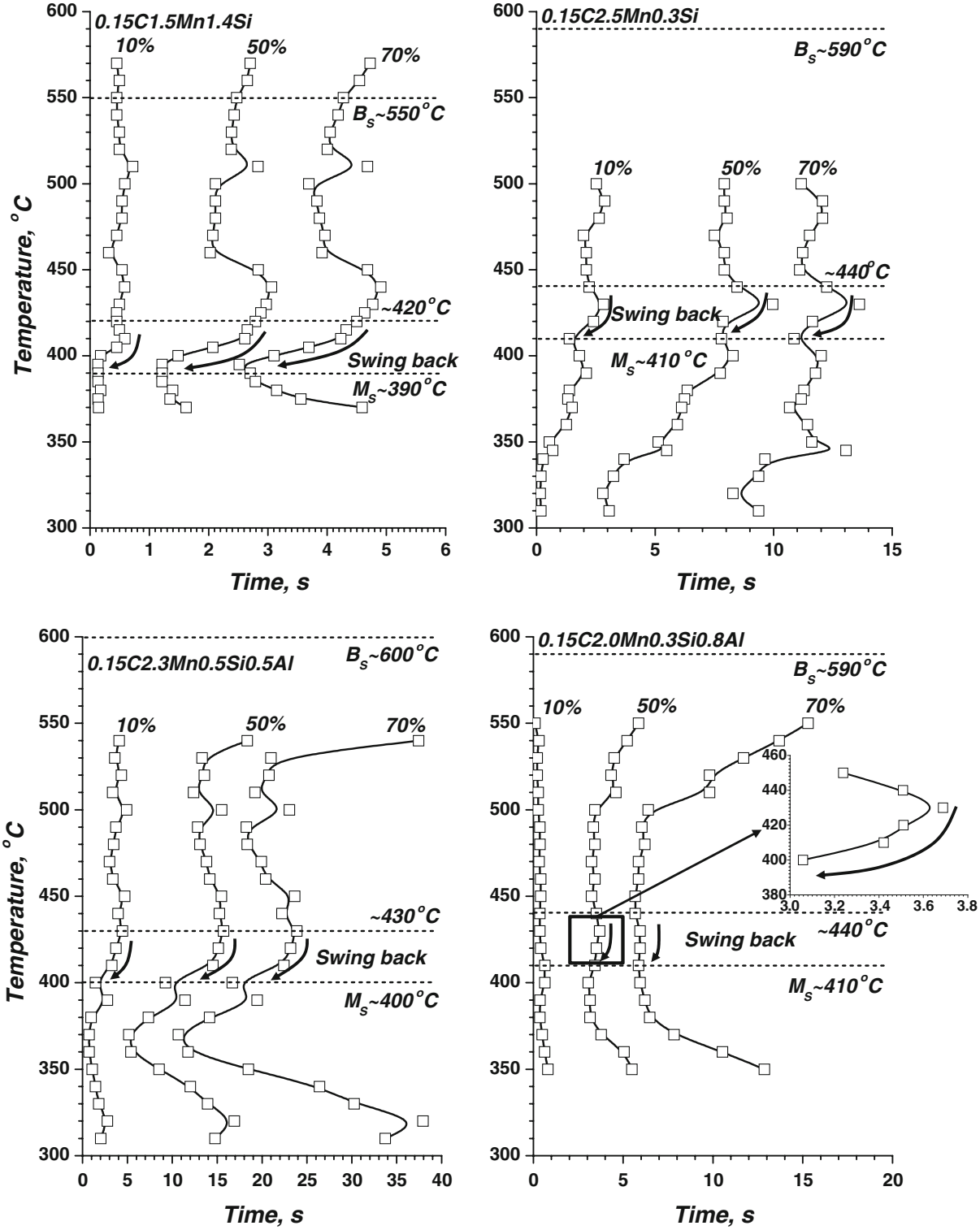


Fig. 3—TTT curves of 0.15C1.5Mn1.4Si, 0.15C2.5Mn0.3Si, 0.15C2.3Mn0.5Si0.5Al, and 0.15C2.0Mn0.3Si0.8Al steels (from upper left to lower right). Note that the phase transformation in the high Si steel was considerably faster and that Al additions retarded the transformation.

0.15C2.0Mn0.3Si0.8Al steel, part of Si was substituted by Al. This substitution resulted in an acceleration of the initial transformation stage. However, as the transformation proceeded, the transformation rate decreased gradually. This was very obvious for the isothermal transformation above 500 °C and below 380 °C. Between 500 °C and 380 °C, the transformation rate was temperature independent. Similar effects were observed for the other two steels. Higher Mn and lower Si contents resulted in a slower transformation in

0.15C2.5Mn0.3Si steel. However, the transformation was accelerated by an increase of the Si and Al contents, as shown for the 0.15C2.3Mn0.5Si0.5Al steel. The clear retardation above 500 °C in the upper bainite transformation range and below 380 °C was also observed.

A "swing back"-type phenomenon, the acceleration of the transformation above the $M_S$ temperature, was typically observed at temperatures about 30 °C above the $M_S$ temperature for the four steels. This phenomenon was originally reported by Radcliffe *et al.* in 1959.[6] The microstructure of the product of the swing back phenomenon was examined in detail by Oka *et al.*[7] They reported that the swing back could be observed either above or below the $M_S$ temperature. They explained the effect by the more rapid onset of the bainite transformation in the case of the swing back phenomenon below the $M_S$ temperature. According to Oka *et al.*, the presence of thin plate-type martensite has an acceleration effect on the nucleation of bainite in the adjacent untransformed austenite.[7] The observed swing back phenomenon has also been described as the formation of a thin platelike isothermal product not belonging to the bainite sequence[8] or the two-stage process consisting of an initial martensite transformation followed by an isothermal bainite transformation.[9]

In the present work, dilatometry data were used to examine the isothermal transformation kinetics above and below the $M_S$ temperature during the one-step Q and P processing of the four steels.

The isothermal transformation data were plotted as $\ln\left(\ln\left(\frac{1}{1-f_{\alpha'}}\right)\right)$ as a function of $\ln t$ (Figure 4), where $f_{\alpha'}$ is the martensite phase fraction and $t$ is the time. Assuming that the transformation data can be fitted to the JMAK equation, $f_{\alpha'} = 1 - \exp(-kt^n)$, the slope of each set of isothermal transformation data represents the exponent, or the $n$ parameter in the JMAK equation.

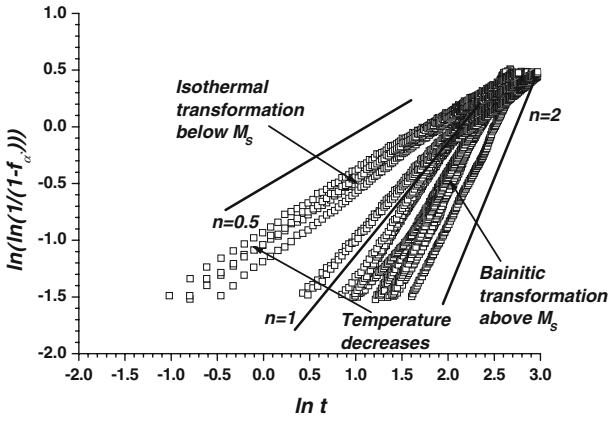


Fig. 4—JMAK equation analysis of the isothermal transformation data for 0.15C2.5Mn0.3Si steel. The slope and $y$ intercept give the value of $n$ and the natural logarithm of the $k$ parameter in JMAK equation, respectively. The $n$ parameter decreases rather sharply when $T_Q$ is below the $M_S$ temperature. The transformation is clearly accelerated in the early stages, despite a clear decrease of the $n$ parameter. In the later stages of the isothermal transformation, the transformation rate decreases gradually.

The temperature dependence of the exponent $n$ is shown in Figure 5. The exponent $n$ displayed only a small temperature dependence above the $M_S$ temperature, *i.e.*, in the bainite transformation temperature range for the four steels. Its value was usually between 1.0 and 1.5 in the temperature range of 400 °C to 500 °C. This value is similar to the value of $n$ for the diffusion-controlled growth of needles or plates with a long dimension.[10] In the case of 0.15C2.0Mn0.3Si0.8Al steel in Figure 5(d), the $n$ parameter decreased for temperatures higher than 500 °C for reasons that have not been examined in more detail because this effect is not directly related to the present focus on isothermal transformation below the $M_S$ temperature. The exponent $n$ decreased clearly when the transformation temperature was below the $M_S$ temperature. This trend was common to all compositions. In the temperature range below the $M_S$ temperature, the value of $n$ was between 0.5 and 1.0. This value has been reported to be linking to a thickening of long needles or plates.[10]

The temperature dependence of the $k$ parameter of the JMAK equation is shown in Figure 6. Generally, the $k$ parameter is given as an Arrhenius-type function, $k = k_0 \exp\left(-\frac{Q}{RT}\right)$.[10] If the isothermal transformation below the $M_S$ temperature is a thermally activated process, the $k$ parameter should decrease continuously as the temperature decreases. The measured $k$ parameter was, however, found to increase sharply close to the $M_S$ temperature. These changes of the values of the $n$ and $k$ parameters clearly indicate that there is a difference in the characteristics of the isothermal bainite transformation above the $M_S$ temperature and the isothermal transformation below the $M_S$ temperature.

The activation energy of the isothermal transformation below the $M_S$ temperature was estimated by linear fitting of the low-temperature $k$ parameter data points marked as black squares in Figure 6 with respect to $\frac{1}{T}$. The activation energies of the isothermal transformation below the $M_S$ temperature were found to be 13.52, 29.96, and 57.34 kJ/mol for the 0.15C1.5Mn1.4Si, 0.15C2.0Mn0.3Si0.8Al, and 0.15C2.3Mn0.5Si0.5Al steels, respectively, which are relatively low values.

The microstructures after athermal martensite transformation, upper bainite transformation at 480 °C, lower bainite transformation at 430 °C, and one-step Q and P steel Q and P at 350 °C are shown in the FE-SEM micrographs of Figure 7 for the 0.15C2.0 Mn0.3Si0.8Al steel. Each microstructure has its own characteristic morphology. The athermal martensite is composed of needlelike martensite laths (***a*** in Figure 7), and isolated polygonal regions are often found at prior austenite grain boundaries (***b*** in Figure 7). In comparison, the isothermally transformed upper and lower bainite contain "granular" bainite (***c*** and ***d*** in Figure 7). The prior austenite grain areas are divided into several blocks of granular bainite, and the small microstructural features in each granular bainite block are aligned parallel along a specific orientation. These microstructural features are finer in the case of lower bainite. The one-step Q and P steel has a more complex microstructure. The microstructure contains martensite laths (***a′*** in Figure 7), which are coarser than the needlelike

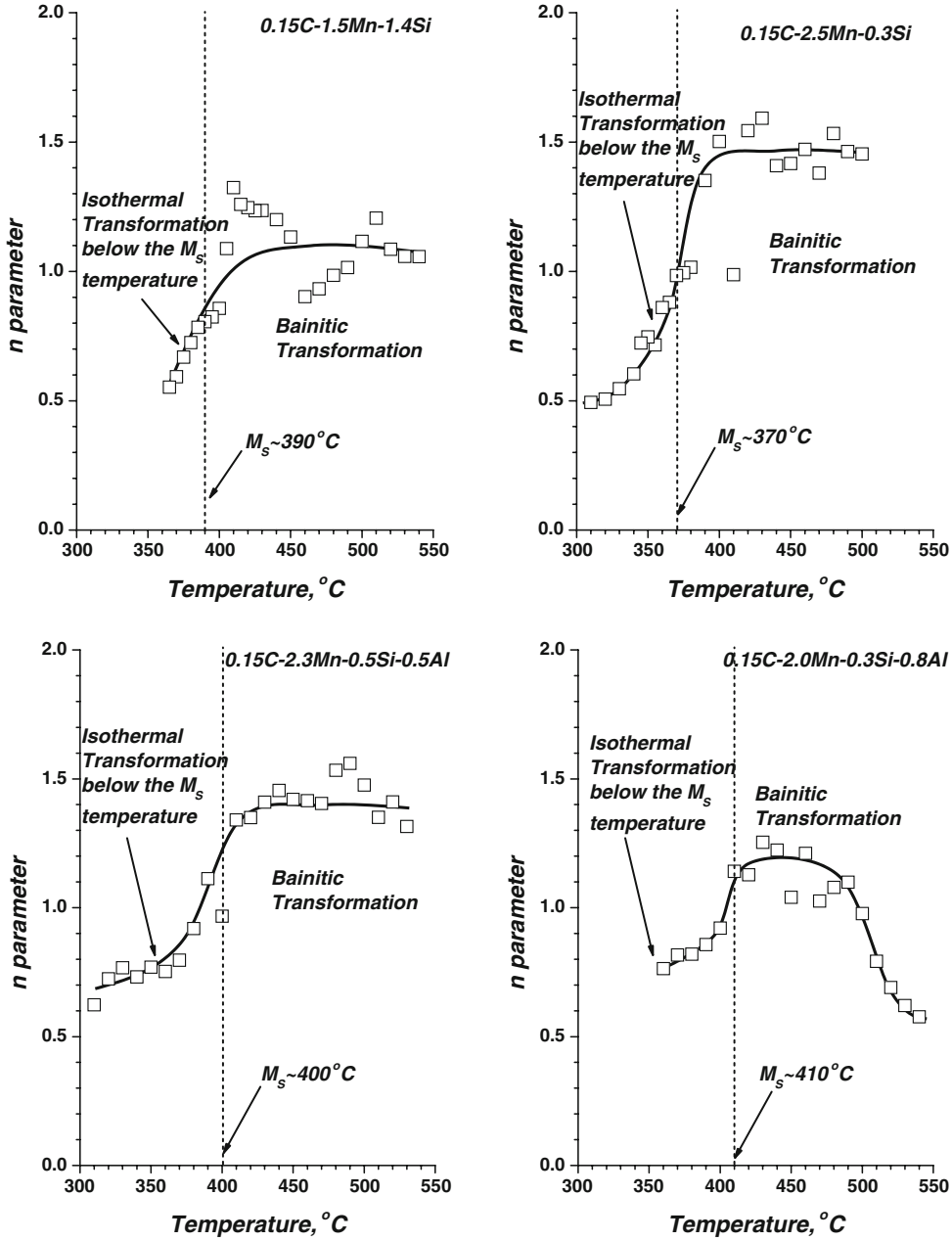


Fig. 5—JMAK equation $n$ parameter for the 0.15C1.5Mn1.4Si, 0.15C2.5Mn0.3Si, 0.15C2.3Mn0.5Si0.5Al, and 0.15C2.0Mn0.3Si0.8Al steels as a function of the quenching temperature. The $n$ parameter had small temperature dependence in the bainite temperature range. When the quenching temperature was below the $M_S$ temperature, the $n$ parameter suddenly decreased to a value less than 1.0.

martensite laths in the athermal martensite (***a*** in Figure 7). The coarser martensite laths in the one-step Q and P steel are thought to be the tempered athermal martensite laths formed during quenching and then tempered during partitioning at the quenching temperature. The polygonal areas (***b′*** in Figure 7), which were found in the athermal martensite (***b*** in Figure 7), are also present at prior austenite grain boundaries. In addition, a complex microstructural feature (***e*** in Figure 7) characteristic of the one-step Q and P steel was found. This feature was not observed in athermal martensite and isothermally transformed bainite. It is believed to be a characteristic product of the isothermal transformation below the $M_S$ temperature. Further microstructure analysis on this morphology is needed to define the characteristics of the isothermal transformation below the $M_S$ temperature in a low-alloyed low-carbon steel.

## IV. DISCUSSION

The main observation of the present work is the isothermal transformation below the $M_S$ temperature during the Q and P process. It is at present not clearly known, however, whether the observed isothermal phase transformation is martensitic or bainitic in nature.

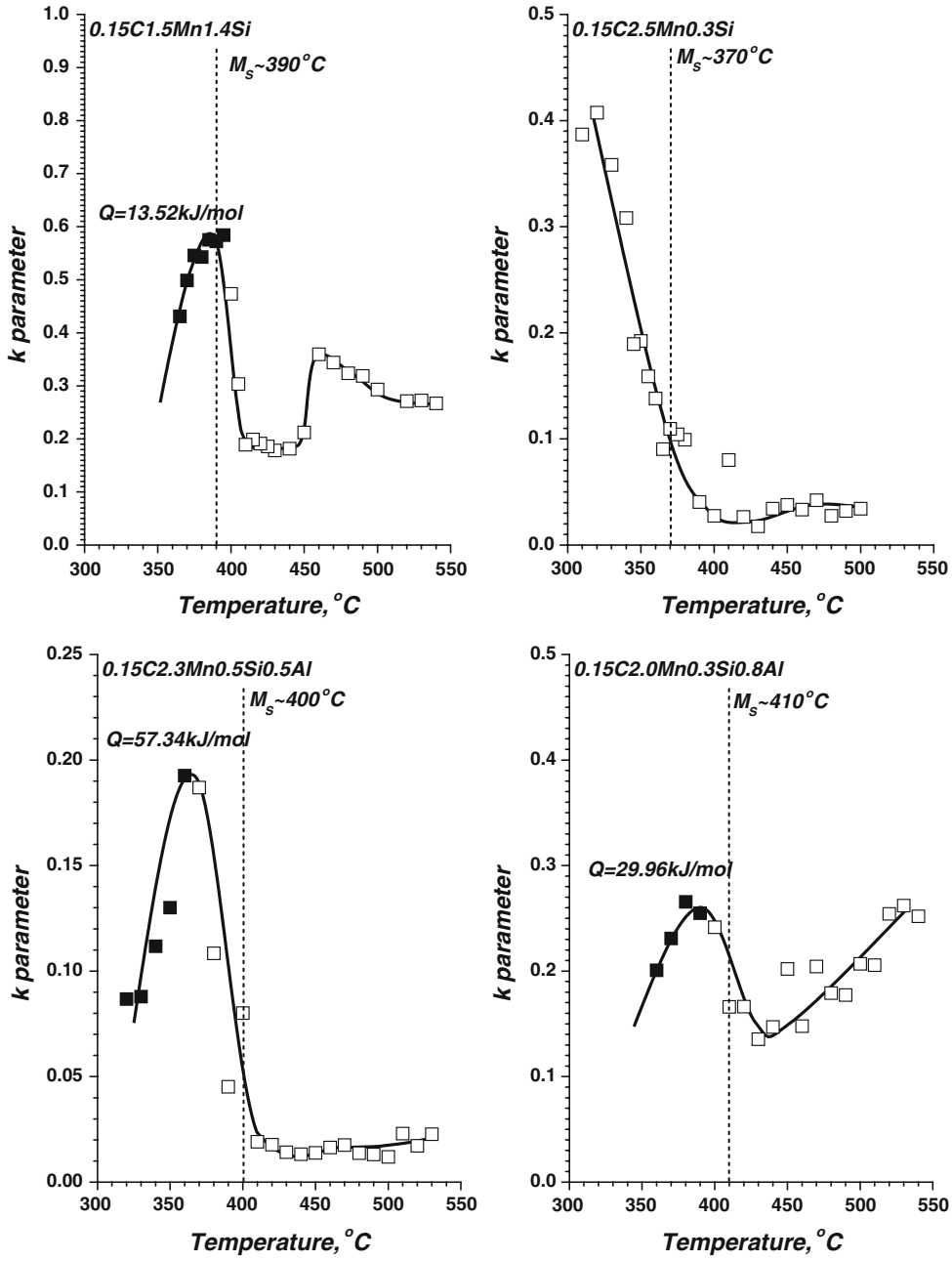


Fig. 6—Trend of $k$ parameter of the 0.15C1.5Mn1.4Si, 0.15C2.5Mn0.3Si, 0.15C2.3Mn0.5Si0.5Al, and 0.15C2.0Mn0.3Si0.8Al steels (from upper left to lower right) with respect to the quenching temperature. The $k$ parameter was sharply increased as the quenching temperature was below the $M_S$ temperature. The black square points below the $M_S$ temperature were selected to calculate the activation energy.

Isothermal transformations in low-alloyed hypo-eutectoid low-carbon steels below the $M_S$ temperature have been reported by only a few authors and the nature of the transformation is still mostly unknown. Averbach and Cohen were the first to report the isothermal decomposition of the austenite into the martensite in a 1.0 mass pct C hyper-eutectoid tool steel.[11] They observed a continuous expansion of a dilatometer sample after quenching to room temperature. They concluded that this expansion was caused by the isothermal decomposition of the retained austenite into martensite. A detailed microstructural analysis, however, was not included in their work. In 1969, Pati and Cohen[12] published results on the nucleation and growth during the early stages of the isothermal martensite transformation in Fe-Mn-Ni alloys. Their work was based on previous work by Kurdjumov and Maksimova.[13] They concluded that the isothermal transformation was martensitic in nature and that the nucleation of the isothermal martensite was affected by autocatalysis due to the elastic and plastic strains in the surrounding austenite caused by the presence of

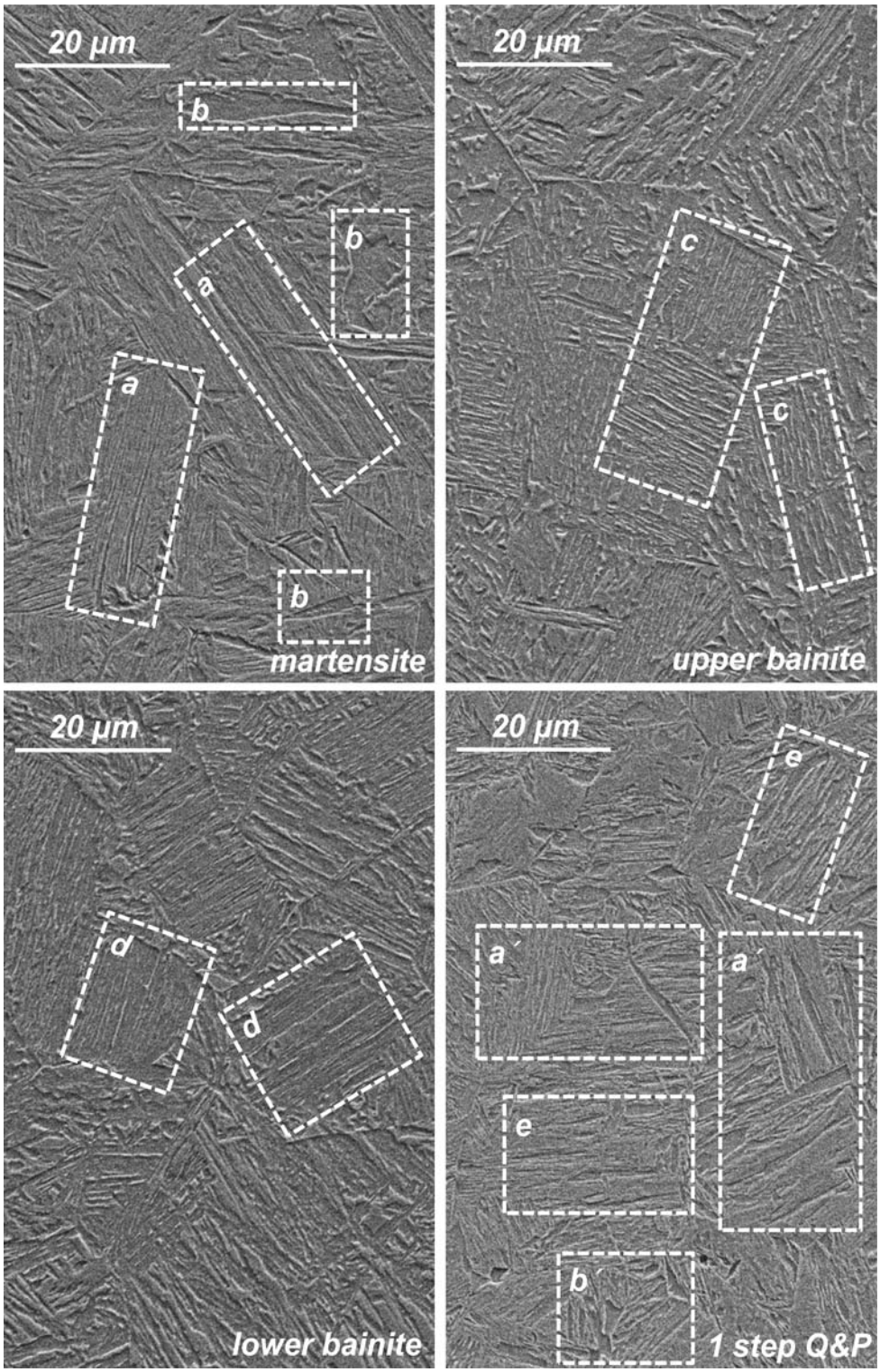


Fig. 7—SEM micrographs of martensite, upper bainite (isothermally transformed at 480 °C), lower bainite (isothermally transformed at 430 °C), and one-step Q and P at 350 °C of 0.15C2.0Mn0.3Si0.8Al steel. Each microstructure has characteristic features labeled a, b, c, d, a′, b′, and e.

martensite. An autocatalytic nucleation model of the isothermal martensite transformation was developed in more detail by the same authors.[14]

Some authors have proposed that the isothermal transformation below the $M_S$ temperature was bainitic in nature. Radcliffe and Rollason[6] observed the swing back phenomenon, *i.e.*, the accelerated isothermal transformation below the $M_S$ temperature in hypereutectoid alloys, and concluded that the more rapid onset of the bainite reaction at temperatures below the

Table II. Compositions, $M_S$ Temperature, and Temperature Range of the Previous Work on the Isothermal Transformation below the $M_S$ Temperature; Generally, the Compositions Were Hyper-Eutectoid or Austenitic Steels with High Mn and Ni

| Authors | Steel Compositions (Wt Pct) | | | | $M_S$ Temperature | Isothermal Transformation Temperature |
|---|---|---|---|---|---|---|
| | C | Mn | Ni | *Etc.* | | |
| Averbach and Cohen[11] | 1.07 | 0.25 | — | 0.23Si | — | 150 °C to 0 °C |
| | 1.00 | 0.37 | | 0.35Si1.56Cr | | |
| Howard and Cohen[8] | 1.35 | — | — | — | — | 315 °C to 177 °C |
| Cech and Hollomon[15] | 0.05 | 3.73 | 22.94 | — | — | −79 °C to −197 °C |
| Radcliffe and Rollason[6] | 0.77 | — | — | — | 264 °C | 450 °C to 186 °C |
| | 1.07 | — | | | 196 °C | |
| | 0.65 | 0.35 | | | 293 °C | |
| Pati and Cohen[12] | 0.017 | 2.98 | 24.20 | — | — | −80 °C to −196 °C |
| Oka and Okamoto[7] | 0.85 | <0.01 | — | — | 273 °C | 328 °C to 167 °C |
| | 1.10 | | | | 231 °C | |
| | 1.45 | | | | 189 °C | |
| | 1.80 | | | | 174 °C | |
| Bohemen *et al.*[16] | 0.66 | 0.69 | — | 0.30Si | 264 °C | 300 °C to 220 °C |
| Present work | 0.15 | 1.50 | — | 1.42Si | 393 °C | 550 °C to 300 °C |
| | 0.15 | 2.50 | | 0.30Si | 367 °C | |
| | 0.15 | 2.32 | | 0.50Si0.50Al | 410 °C | |
| | 0.15 | 2.00 | | 0.30Si0.80Al | 400 °C | |

$M_S$ temperature was a "well-established phenomenon." They argued that the transformation acceleration was due to the effect of the presence of martensite plates on the nucleation of bainite in adjacent regions of untransformed austenite. Oka and Okamoto[7] investigated the transformation kinetics and microstructure of the austenite decomposition around the $M_S$ temperature in hyper-eutectoid steels. By means of transmission electron microscopy, they showed the existence of thin plate or lathlike isothermal martensite. They also reported the presence of the lower bainite with midrib.

From these studies, no single mechanism for the nature of the isothermal transformation below the $M_S$ temperature can be extracted. The relevant publications on the isothermal transformation below the $M_S$ temperature are listed in Table II.

The isothermal austenite decomposition below the $M_S$ temperature has often been examined mainly in order to clarify the mechanisms of the isothermal transformation. Much of the work done on the isothermal transformation therefore has been done in high carbon, often hyper-eutectoid, or highly Ni alloyed steels. The use of these ferrous alloys makes it possible to observe the relatively slow growth of the isothermal martensite in isolation at relatively low temperatures. The study of the isothermal martensite transformation in low-carbon steel is more difficult because the prior athermal martensite formation cannot be avoided.

The JMAK equation parameter analysis (Figures 5 and 6), however, showed that there was a clear difference between the isothermal transformation above the $M_S$ temperature, *i.e.*, in the bainite formation temperature range, and the isothermal transformation below the $M_S$ temperature. The sharp decrease of the $n$ parameter and the sharp increase of the $k$ parameter for temperatures close to the $M_S$ temperature, and the small activation energy associated with the transformation, clearly suggest that the isothermal transformation below the $M_S$ temperature is not a low-temperature continuation of the bainite decomposition reaction. The activation energies required for the isothermal transformation below the $M_S$ temperature obtained for 0.15C1.5Mn1.4Si, 0.15C2.0Mn0.3Si0.8Al, and 0.15C2.3Mn0.5Si0.5Al steels were 13.52, 29.96, and 57.34 kJ/mol, respectively. These activation energies are lower than the activation energies of ~100 kJ/mol usually reported for diffusion-controlled processes.[10] Isothermal martensite transformation activation energy values reported in the literature are listed in Table III. In these reports, the low activation energy is usually ascribed to the movement of interfacial dislocations,[21] the movement of the thermally activated partial dislocations,[22] or the nucleation of the martensite.[14,23]

Borgenstam *et al.* reported a relatively high activation energy of ~80 kJ/mol for a Fe-Ni alloy with less than 0.005 mass pct carbon. They noticed that this value was similar to the activation energy for the bainite transformation in hyper-eutectoid steels for which the bainite transformation includes carbon diffusion and that the crystallography of the isothermal transformation product in a Fe-Ni alloy was related to the formation of bainite.[24] They concluded that this high activation energy was due to a slowly nucleated diffusionless bainite transformation, which grows very rapidly. The lower activation energies also imply that the isothermal transformation observed in the present work may not be a diffusion-controlled process. Instead, these low activation energies are thought to be related, not to a diffusion-controlled transformation, but to the movement of transformation dislocations formed during the isothermal transformation below the $M_S$ temperature.

It is well known that a higher activation energy results in a slower transformation rate for a thermally activated transformation.[10] In the present work, the 0.15C1.5Mn1.4Si steel had the lowest activation energy for the isothermal transformation below the $M_S$

**Table III. Composition, Activation Energy, and Expected Mechanism for the Transformation; in Most of the Prior Work, it is Argued That Low Activation Energies are Related to Mechanisms Related to the Movement of Transformation Dislocations**

| Authors | Composition | Activation Energy | Transformation Mechanism |
|---|---|---|---|
| Lement *et al.*[20] | commercial steel with 0.6 to 1.4 wt pct C | ~113 kJ/mol | C diffusion interacting with the partial dislocation |
| Pati *et al.*[14] | Fe-24Ni-3Mn | ~42 kJ/mol | nucleation for the isothermal martensite |
| Yang *et al.*[21] | Fe-21Ni-4Mn | ~59 kJ/mol | movement of the interfacial dislocations |
| Ghosh *et al.*[22] | Fe-23.2Ni-2.8Mn | ~29 to 140 kJ/mol | thermally activated motion of the partial dislocations |
| Thadhani *et al.*[23] | Fe-32Ni-0.035C | ~105 to 160 kJ/mol | interface-mobility controlled nucleation |
| Borgenstam *et al.*[24] | Fe-Ni-(Cr,Mn) | ~7 kJ/mol | slip or twinning |
| | Fe-C-X | ~80 kJ/mol | diffusion of the carbon atoms |
| | Fe-Ni (no carbon) | ~80 kJ/mol | related to the bainite transformation |
| Van Bohemen *et al.*[16] | Fe-0.66C | ~43 kJ/mol | bainite transformation |
| Present work | 0.15C1.5Mn1.4Si | ~13 kJ/mol | neither pure bainitic nor martensitic in nature |
| | 0.15C2.0Mn0.3Si0.Al | ~25 kJ/mol | |
| | 0.15C2.3Mn0.5Si0.5Al | ~57 kJ/mol | |
| | 0.15C2.5Mn0.3Si | — | |

temperature and also the shortest elapsed time for a specific fraction of transformation product. The 0.15C2.3Mn0.5Si0.5Al steel had the highest activation energy for the isothermal transformation below the $M_S$ temperature and a much longer time was needed to obtain a same amount of the transformation product.

An additional complicating aspect of studying isothermal martensite in hypo-eutectoid steels is the unavoidable presence of athermal martensite. The presence and the amount of prior athermal martensite at the quenching temperature might contribute, by, *e.g.*, autocatalytic nucleation, to the change of the transformation kinetics. The isothermal transformation rates during the nucleation stage and in the growth stage were therefore compared to examine the effect of the existence of the prior athermal martensite.

The simplified relation between the transformation rate in the nucleation stage of the isothermal martensite transformation can be derived on the basis of the following equation for the nucleation rate of an isothermal transformation:[17,18]

$$\dot{N} = N_i v \exp(-Q/\mathrm{R}T) \qquad [1]$$

where $\dot{N}$ is the number of nuclei/s·cm$^3$, $N_i$ is the number of preferred sites/cm$^3$ at which the initial martensite plates are nucleated, $v$ is the lattice vibration frequency, and $Q$ is the activation energy for the nucleation. The term R is the gas constant and $T$ is the absolute temperature.

If a martensite volume fraction increase, $\Delta f$, is detected in a time interval $\Delta t$, one obtains

$$\Delta f = \dot{N} V_\alpha \Delta t \qquad [2]$$

where $V_\alpha$ is the initial martensite plate volume.Combining Eqs. [1] and [2], one finds

$$\ln\left(\dot{N} V_\alpha\right) = \ln\left(\frac{\Delta f}{\Delta t}\right) = \ln(N_i v_i v) - \frac{Q}{\mathrm{R}T} \qquad [3]$$

where ln ($N_i v_i v$) can be assumed constant.[17] The natural logarithm of the transformation rate (Figure 8), $\ln\left(\frac{\Delta f}{\Delta t}\right)$,

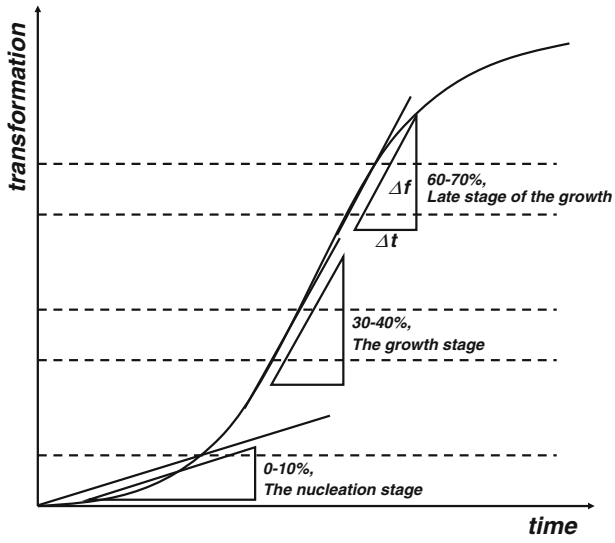


Fig. 8—Schematic of the isothermal transformation *vs* time curve and the data selection. The nucleation, growth, and late stages of the growth were selected to examine the effect of the prior athermal martensite.

was plotted as a function of the amount of prior athermal martensite (Figure 9) and the reciprocal temperature (Figure 10). The amount of prior athermal martensite was controlled by varying the quenching temperature.

For a clear understanding of Figure 9, Figure 9(b) should be considered first. This figure shows that the initial nucleation-related rate of transformation increases as the fraction of prior athermal martensite increases. However, the late growth stage related transformation rate decreases. For Figure 9(a), a similar tendency was observed, except that, in the late growth stage of the isothermal transformation, there is a slight increase at low prior athermal martensite fraction and a decrease at high athermal martensite fraction.

For CMnSiAl compositions, the situation is more complex. For Figure 9(c), the transformation rate was increased by the existence of ~10 pct volume fraction of

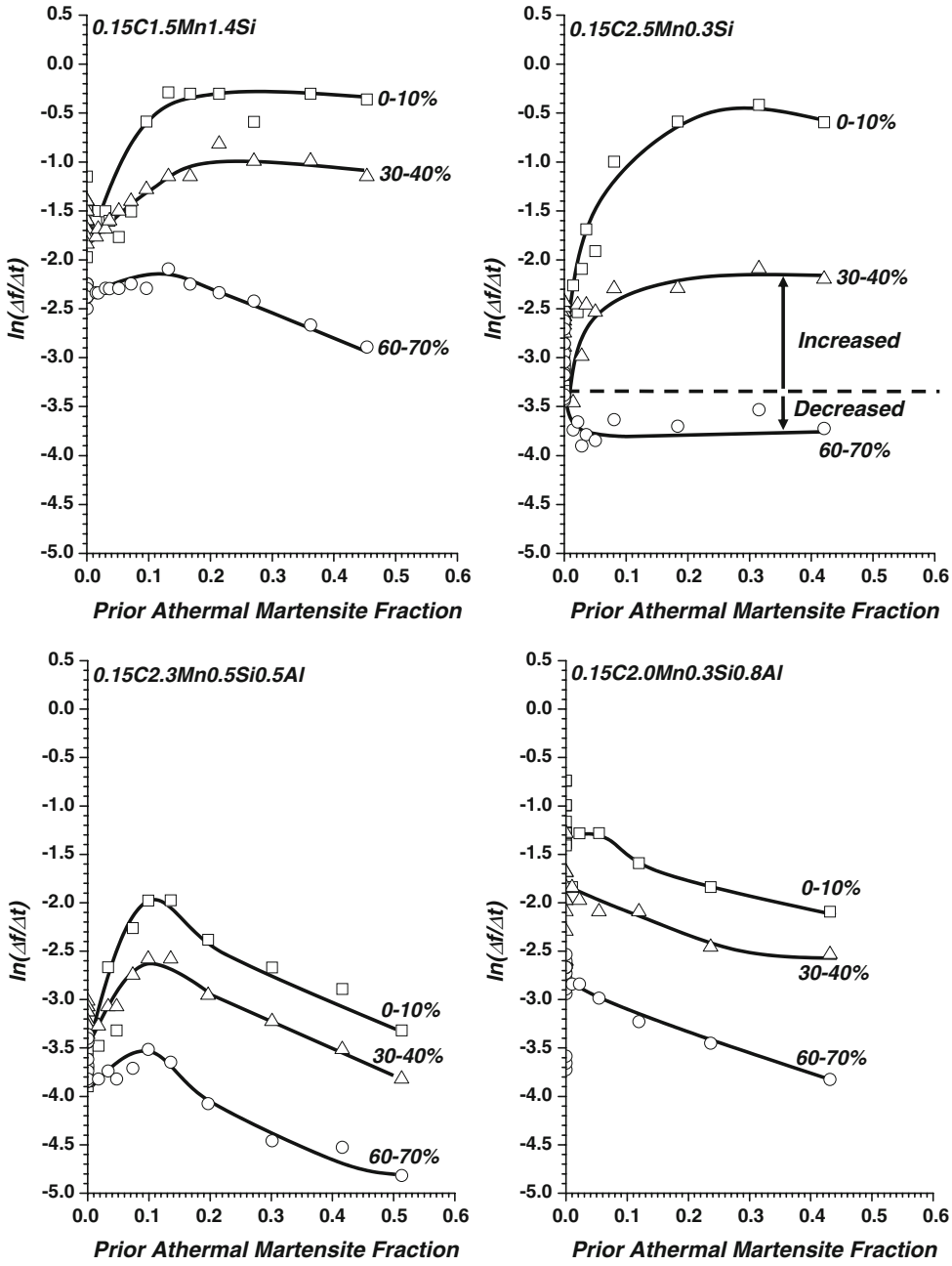


Fig. 9—Transformation rate of the 0.15C1.5Mn1.4Si, 0.15C2.5Mn0.3Si, 0.15C2.3Mn0.5Si0.5Al, and 0.15C2.0Mn0.3Si0.8Al steels (from upper left to lower right) with respect to the prior athermal martensite fraction. The prior athermal martensite accelerated the nucleation stage of the isothermal transformation below the $M_S$ temperature.

prior athermal martensite in 0.15C2.3Mn0.5Si0.5Al steel. When the volume fraction of prior athermal martensite exceeded 10 pct, the rate of the isothermal transformation decreased. For Figure 9(d), the rate of the isothermal transformation always decreased. The late growth stage was more strongly suppressed.

The increase of the isothermal transformation rate in the presence of a small volume fraction of prior athermal martensite in two CMnSi steels could be explained by the autocatalytic nucleation caused by the effect of the stress or strain field of the prior athermal martensite on the transformation of the austenite. However, the martensite embryos, which require relatively low driving force for transformation, could already have been consumed during the prior athermal martensite transformation. The transformation accelerating effect of prior athermal martensite, therefore, would be compensated and the transformation rate might be maintained constant despite the increasing amount of the prior athermal martensite. The situation is more complex in the case of the CMnSiAl steels. The existence of prior athermal martensite resulted in a decreased transformation rate in the Al-added steels. This may be due to the Al additions, which may slow

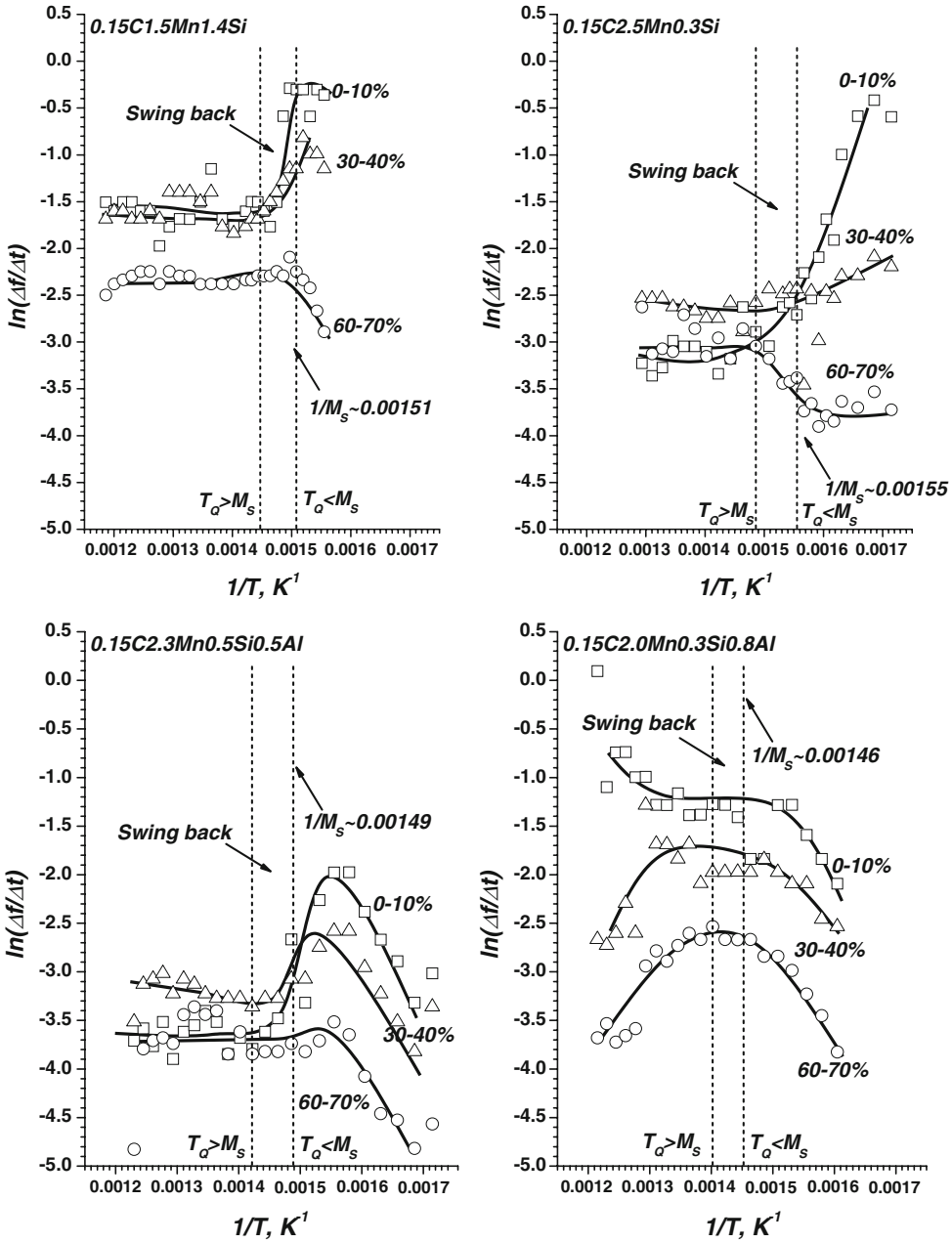


Fig. 10—Transformation rate of the 0.15C1.5Mn1.4Si, 0.15C2.5Mn0.3Si, 0.15C2.3Mn0.5Si0.5Al, and 0.15C2.0Mn0.3Si0.8Al steels (from upper left to lower right) with respect to the $1/T$. In the CMnSi class steel, the initial stage of the transformation was accelerated and the late stage of the transformation was retarded as the quenching temperature was below the $M_S$ temperature. In CMnSiAl steel, the initial stage of the transformation was accelerated; however, further decrease of the quenching temperature also retarded the transformation.

either the partitioning of carbon atoms to untransformed austenite or the formation of transition carbides during prior athermal martensite formation.[19]

During the Q and P process, quenching is interrupted at a temperature between the $M_S$ and $M_f$ temperatures. The carbon can partition from the prior athermal martensite into the untransformed austenite at a quenching temperature high enough to allow for carbon diffusion. During the isothermal transformation at the quenching temperature, carbon atoms in the prior athermal martensite and in the fresh isothermal transformation product can partition to the untransformed austenite or contribute to transition carbide formation. The kinetics of the carbon atom transfer to untransformed austenite is gradually slower when the amount of remaining austenite is continuously reduced. This mechanism is thought to retard the transformation at higher athermal volume fractions.

The change of the transformation rate with respect to the inverse of the quenching temperature is shown in Figure 10. The accelerated initial transformation stage and the slower later stage of the isothermal transformation below the $M_S$ temperature are also clear in this plot. In the two CMnSi steels, the initial transformation

rate corresponding to the 0 to 10 pct isothermal transformation increased sharply because the quenching temperature was below the $M_S$ temperature. The transformation rate of the 30 to 40 pct transformation also increased as the quenching temperature decreased, but not as much as in the 0 to 10 pct transformation range. In contrast, the transformation rate decreased in the late stage of the transformation even at lower quenching temperatures. In the two CMnSiAl steels, the transformation rate in the nucleation stage increased when the quenching temperature was close to the $M_S$ temperature, *i.e.*, in conditions of small amounts of prior athermal martensite. The transformation rate decreased when the quenching temperature decreased further.

Figure 11 shows a schematic comparison between the athermal martensite transformation and the isothermal transformation below the $M_S$ temperature. During athermal martensite formation, the time required for carbon diffusion from a martensite lath to retained interlath austenite is approximately $2.37 \cdot 10^{-3}$ s in a low-carbon steel.[25–28] In comparison, the time required for the formation of a low-carbon martensite lath is ~$10^{-7}$ to $10^{-5}$ seconds.[29,30] The diffusion of carbon during the formation of athermal lath martensite, therefore, can only keep pace with the formation of the martensite at lower cooling rates. In general, however, because the martensite transformation is much faster than the carbon diffusion, the carbon atoms remain in the interstitial sites and the transformation will be fully diffusionless. In contrast, during the isothermal transformation of low-carbon steels below the $M_S$ temperature, the carbon atoms can diffuse out of the prior athermal martensite into the adjacent untransformed austenite if the quenching temperature is high enough. The austenite can then be continuously enriched in carbon, and untransformed austenite will decompose by a mechanism that is neither purely martensitic nor bainitic. The simultaneous growth of the prior athermal martensite laths may result in the additional complexity of the isothermal transformation of low-carbon steels below the $M_S$ temperature.

## V. CONCLUSIONS

Dilatometry data have revealed that, when a Q and P heat treatment is carried out on low-alloy low-carbon steels, an isothermal transformation is clearly observed when the quenching is interrupted between the $M_S$ and $M_f$ temperatures. The $n$ and $k$ parameters in the JMAK equation revealed that there was a change in the nature of the transformation from a bainite transformation to a more complex isothermal transformation below the $M_S$ temperature. The precise nature of the isothermal transformation below the $M_S$ temperature is still unclear at present.

In the TTT curves, the swing back phenomenon was clearly observed in the temperature range between the $M_S$ temperature and about 30 °C above the $M_S$ temperature. The effects of Mn, Si, and Al on the isothermal transformation could be compared. A relatively high Mn content retarded the isothermal transformation in 0.15C2.5Mn0.3Si and 0.15C2.3Mn0.5Si0.5Al steels. A large concentration of Si is known to retard the formation of the cementite from austenite, resulting in the carbide-free microstructure[19] or epsilon carbide formation.[25] The FE-SEM images show a reduced amount of the carbide in the microstructure of the one-step Q and P steel. When Si was partially substituted by Al, the transformation kinetics became more complex.

The prior athermal martensite transformed during quenching to the temperature between the $M_S$ and $M_f$ temperatures accelerated the isothermal transformation. In CMnSi steels, the transformation rate of the early stages during the isothermal transformation below the $M_S$ temperature was strongly accelerated by the existence of the prior athermal martensite. In CMnSiAl steels, however, a small amount of the prior athermal

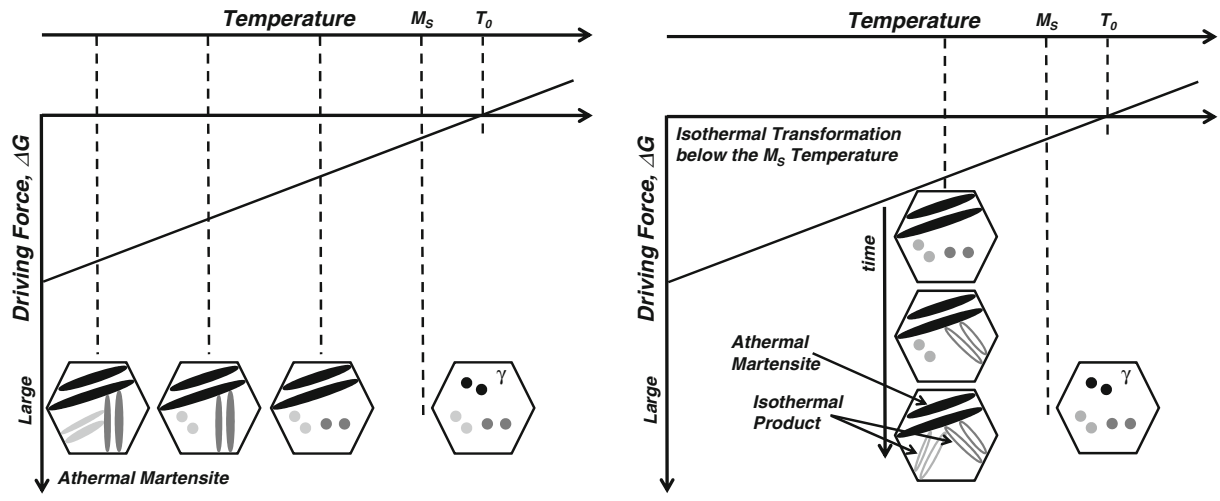


Fig. 11—Schematic comparison between the athermal martensite transformation (left) and isothermal transformation below the $M_S$ temperature. During the isothermal transformation below the $M_S$ temperature, the carbon can diffuse into the adjacent untransformed austenite and it results in a more complex decomposition of the untransformed austenite.

martensite, about 10 vol pct, accelerated the transformation rate of the isothermal transformation below the $M_S$ temperature. The transformation rate decreased, however, with increased amount of the prior athermal martensite.

## ACKNOWLEDGMENT

The authors gratefully acknowledge the support of POSCO (Pohang, South Korea) and ASPPRC (Colorado School of Mines, Golden, CO).

## REFERENCES

1. D.V. Edmonds, K. He, F.C. Rizzo, B.C. De Cooman, D.K. Matlock, and J.G. Speer: *Mater. Sci. Eng. A*, 2006, vols. 438–440, pp. 25–34.
2. A.J. Clarke, J.G. Speer, M.K. Miller, R.E. Hackenberg, D.V. Edmonds, D.K. Matlock, F.C. Rizzo, K.D. Clarke, and E. De Moor: *Acta Mater.*, 2008, vol. 56 (1), pp. 16–22.
3. J.G. Speer, D.K. Matlock, B.C. De Cooman, and J.G. Schroth: *Acta Mater.*, 2003, vol. 51 (9), pp. 2611–22.
4. D.P. Koistinen and R.E. Marburger: *Acta Metall.*, 1959, vol. 7 (1), pp. 59–60.
5. S.J. Kim, H.S. Kim, and B.C. De Cooman: *AIST Steel Properties and Applications Conference Proceedings*, MS&T'07, Detroit, 2007, pp. 73–83.
6. S.V. Radcliffe and E.C. Rollason: *J. Iron Steel Inst.*, 1959, vol. 191, pp. 56–65.
7. M. Oka and H. Okamoto: *Metall. Trans. A*, 1988, vol. 19A, pp. 447–52.
8. R.T. Howard and M. Cohen: *Trans. AIME*, 1948, vol. 176, pp. 384–400.
9. O. Schaaber: *Trans. AIME*, 1955, vol. 203, pp. 559–60.
10. J.W. Christian: *The Theory of Transformations in Metals and Alloys*, 2nd ed., Elsevier Science Ltd., New York, NY, 2001, p. 546.
11. B.L. Averbach and M. Cohen: *Trans. ASM*, 1949, vol. 41, pp. 1024–60.
12. S.R. Pati and M. Cohen: *Acta Metall.*, 1969, vol. 17, pp. 189–99.
13. G.V. Kurdjumov and O.P. Maksimova: *Dokl. Akad. Nauk. SSSR*, 1948, vol. 61, pp. 83–93.
14. S.R. Pati and M. Cohen: *Acta Metall.*, 1971, vol. 19, pp. 1327–32.
15. R.E. Cech and J.H. Hollomon: *Trans. AIME*, 1953, vol. 197, pp. 685–89.
16. S.M.C. van Bohemen, M.J. Santofimia, and J. Sietsma: *Scripta Mater.*, 2008, vol. 58, pp. 488–91.
17. C.H. Shih, B.L. Averbach, and M. Cohen: *Trans. AIME*, 1955, vol. 203, pp. 183–87.
18. T.Y. Hsu, Y. Chen, and W. Chen: *Metall. Trans. A*, 1987, vol. 18A, pp. 1531–32.
19. H.K.D.H. Bhadeshia: *Bainite in Steels: Transformations, Microstructures and Properties*, 2nd ed., IOM Communications Ltd., London, 2001, p. 73.
20. B.S. Lement and M. Cohen: *Acta Metall.*, 1956, vol. 4 (5), pp. 469–76.
21. D. Z. Yang and C.M. Wayman: *Acta Metall.*, 1984, vol. 32 (6), pp. 949–54.
22. G. Ghosh and V. Raghavan: *Mater. Sci. Eng.*, 1986, vol. 80 (1), pp. 65–74.
23. N.N. Thadhani and M.A. Meyers: *Acta Metall.*, 1986, vol. 34 (8), pp. 1625–41.
24. A. Borgenstam and M. Hillert: *Acta Mater.*, 1997, vol. 45 (2), pp. 651–62.
25. T.Y. Hsu, X. Zuyao, and L. Xuemin: *Scripta Metall.*, 1983, vol. 17 (11), pp. 1285–88.
26. C. Wells and R.F. Mehl: *Trans. AIME*, 1940, vol. 140, pp. 279–306.
27. B.V. Rao and G. Thomas: *Proc. ICOMAT-79*, Massachusetts Institute of Technology, Cambridge, MA, 1979, pp. 12–19.
28. G. Thomas and M. Sarikaya: *Proc. Int. Conf. on Solid-Solid Phase Transformations*, TMS-AIME, Warrendale, PA, 1982, pp. 999–1003.
29. J.M. Marder and A.R. Marder: *Trans. ASM*, 1969, vol. 62, pp. 1–10.
30. R.B.G. Yeo: *Trans. ASM*, 1964, vol. 57, pp. 48–61.